Chemistry and Physics of Lipids 183 (2014) 91–99

Contents lists available at ScienceDirect

Chemistry and Physics of Lipids

journal homepage: www.elsevier.com/locate/chemphyslip

Conditions for liposome adsorption and bilayer formation on BSA passivated solid supports

Elsa I. Silva-López [a], Lance E. Edens [b], Adam O. Barden [a], David J. Keller [b], James A. Brozik [a,*]

[a] Department of Chemistry, Washington State University, PO Box 644630, Pullman, WA 99164-4630, United States
[b] Department of Chemistry and Biological Chemistry, University of New Mexico, Albuquerque, NM 87131–0001, United States

ARTICLE INFO

Article history:
Received 20 March 2014
Received in revised form 2 June 2014
Accepted 4 June 2014
Available online 6 June 2014

Keywords:
Planar lipid bilayer
Bovine serum albumin
Beta mercaptoethanal
Diffusion
FRAP
AFM

ABSTRACT

Planar solid supported lipid membranes that include an intervening bovine serum albumen (BSA) cushion can greatly reduce undesirable interactions between reconstituted membrane proteins and the underlying substrate. These hetero-self-assemblies reduce frictional coupling by shielding reconstituted membrane proteins from the strong surface charge of the underlying substrate, thereby preventing them from strongly sticking to the substrate themselves. The motivation for this work is to describe the conditions necessary for liposome adsorption and bilayer formation on these hetero-self-assemblies. Described here are experiments that show that the state of BSA is critically important to whether a lipid bilayer is formed or intact liposomes are adsorbed to the BSA passivated surface. It is shown that a smooth layer of native BSA will readily promote lipid bilayer formation while BSA that has been denatured either chemically or by heat will not. Atomic force microscopy (AFM) and fluorescence microscopy was used to characterize the surfaces of native, heat denatured, and chemically reduced BSA. The mobility of several zwitterionic and negatively charged lipid combinations has been measured using fluorescence recovery after photobleaching (FRAP). From these measurements diffusion constants and percent recoveries have been determined and tabulated. The effect of high concentrations of beta-mercaptoethanol (β-ME) on liposome formation as well as bilayer formation was also explored.

1. Introduction

It is often advantageous to study biological molecules (proteins, DNA, RNA, biological membranes, etc.) in the absence of other cellular components. This can be challenging for membrane proteins because the membrane is essential to both structure and overall function. For these reasons, isolated membrane proteins are often studied as reconstituted constituents within self-assembled bilayers, liposomes, or in amphiphilic polymers that mimic a membrane. Many model membrane systems have been developed, and provide a conceptually simple experimental setting that is ideal for the study of biological activity at the surface of membranes, within lipid bilayers, or across lipid membranes (Castellana and Cremer, 2006; Chan and Boxer, 2007; Fruh et al., 2011; Rigaud and Levy, 2003).

The deposition of lipid vesicles and the formation of supported lipid bilayers is governed by many interactions, including the interaction between lipid vesicles and the solid support, nearest neighbor interactions between adsorbed vesicles, and molecular interactions within individual adsorbed vesicles (Cremer and Boxer, 1999; Johnson et al., 2002; Keller et al., 2000; Lipowsky and Seifert, 1991a,b; Rabe et al., 2011; Reimhult et al., 2002, 2003; Reviakine and Brisson, 2000; Tribet and Vial, 2008; Zhdanov and Kasemo, 2001). In order for adsorbed vesicles to form a continuous lipid bilayer they must first rupture, which occurs only after a deformation exceeds a given threshold (Richter et al., 2006; Richter et al., 2003). The stability and mobility of the newly formed supported lipid bilayer is controlled by steric and van der Waals forces, hydrogen bonding, and electrostatic interactions (Castellana and Cremer, 2006; Jelinek and Silbert, 2009; Rigaud and Levy, 2003; Tresset, 2009). Membrane fluidity is maintained by a 10–30 Å layer of trapped water (buffer) between the substrate and the lipid bilayer (Hartshorn et al., 2010; Johnson et al., 1991; Kim et al., 2001).

A major concern when studying reconstituted transmembrane proteins is the proximity to the solid support. For instance, the distance between the membrane and the solid support is, under most circumstances, not large enough to avoid direct contact between a reconstituted transmembrane protein and the

* Corresponding author. Tel.: +1 5093353746; fax: +1 5093358867.
E-mail address: brozik@wsu.edu (J.A. Brozik).

http://dx.doi.org/10.1016/j.chemphyslip.2014.06.002
0009-3084/

underlying substrate. This is significant because contact with the substrate can decrease protein mobility, function, and can even lead to denaturation (Johnson et al., 1991; Wagner and Tamm, 2000). To overcome this problem, "cushions" and "tethers" have been developed to separate the lipid bilayer from the underlying solid support as well as reduce the frictional coupling experienced by reconstituted proteins (Diaz et al., 2008; Tanaka and Sackmann, 2005; Wagner and Tamm, 2000). By way of definitions, a cushion is a polymer/oligomer (natural or synthetic) that sits between a bilayer and a solid support and is either pinned at one end to the membrane or the substrate, or not pinned at all. A tether sits between a lipid bilayer and solid support with one end strongly attached to the membrane (a constituent lipid molecule, integral membrane protein, cholesterol, etc.) and the other strongly attached to the substrate.

Formation of a cushion is normally achieved through either adsorption or covalent grafting onto a solid support or by covalent attachment to a membrane component. Tethering is achieved by reacting a modified surface with chemically functionalized lipids, proteins, or other lipophilic moieties (Cornell et al., 1997; Han et al., 2009; Kendall et al., 2010; Sackmann, 1996). It is believed that cushions and tethers act as a 'lubricating' layer between the membrane and the solid support, mimicking extracellular components or a cell's glycocalyx (Diaz et al., 2008; Sackmann and Tanaka, 2000; Tanaka and Sackmann, 2005; Tribet and Vial, 2008; Wagner and Tamm, 2000,b; Wong et al., 1999a,b). Some examples include the use of dextran (Elender et al., 1996; Kuhner and Sackmann, 1996), cellulose (Goennenwein et al., 2003), branched polyethyleneimine (PEI) (Majewski et al., 1998; Wong et al., 1999a,b), and polyethyleneglycol (PEG) (Albertorio et al., 2005; Kaufmann et al., 2009; Merzlyakov et al., 2006; Munro and Frank, 2004; Wagner and Tamm, 2000). Modifications of these approaches include tethering two lipid bilayers to one another and multiple cushions yielding assemblies with enhanced fluidity and membrane protein mobility (Diaz et al., 2008; Kunding and Stamou, 2006; Murray et al., 2009; Sumino et al., 2011). In addition, the use of tethers and cushions allows for some control of the distance between the solid support and lipid bilayer (Chung et al., 2009; Diaz et al., 2008; Kunding and Stamou, 2006; Sumino et al., 2011).

A common cushion used in the study of purified and reconstituted membrane proteins includes BSA adsorbed to a hydrophilic surface together with a PEGylated lipid bilayer formed by fusion of PEGylated liposomes or proteoliposomes. When BSA is incorporated into a hetero-self-assembly, its function is quite different than other cushions and tethers. BSA adsorbs strongly and uniformly coats hydrophilically treated surfaces. It is unique because it passivates the surface but still maintains enough surface charge itself to promote bilayer formation and does not increase surface roughness greatly (Diaz et al., 2008). It also contains Ca^{++} chelation sites necessary for lipid bilayer formation when negatively charged lipid components are used. The major result of this study is that the state of BSA is critically important to bilayer formation via vesicle fusion irrespective of overall surface coverage. The article also explores the effects of beta-mercaptoethanol on liposome formation, size distribution, and bilayer formation. Given the growing interest in the use of cushioned lipid bilayers containing BSA and our own observations of its finicky behavior, these results may explain some of the divergent behavior found in earlier results using BSA cushions.

2. Materials and methods

2.1. Materials

1-palmitoyl-2-oleoyl-*sn*-glycero-3-phosphocholine (POPC), 1-palmitoyl-2-oleoyl-sn-glycero-3-[phospho-rac-(1-glycerol)] (POPG), 1,2-dimyristoyl-*sn*-glycero-3-phosphocholine (DMPC), L-α-phosphatidylserine (sodium salt) (Brain-PS), 1,2-dioleoyl-*sn*-glycero-3-phosphoethanolamine-*N*-[methoxy(polyethylene glycol)-2000] (ammonium salt) (PEG2000-PE), and 1,2-dimyristoyl-*sn*-glycero-3-phosphoethanolamine-*N*-(lissamine rhodamine B sulfonyl) (ammonium salt) (Liss Rhod-PE) were purchased from Avanti Polar Lipids. Bovine serum albumin (BSA) (Sigma–Aldrich; 99%) was used without further purification. BSA conjugated with tetramethyrhodamine (BSA-TMR) was purchased from Life Technologies Inc. and used as received. All aqueous solutions were prepared from water that was purified using a NANOpure Ultrapure water filtration system (Barnstead, Dubuque, IA) with a minimum resistivity of 18.2 MΩ. Samples free of β-Mercaptoethanol (β-ME) were prepared in four different buffer systems: (1) 10 mM HEPES (EMD chemicals), (2) 10 mM Phosphate Buffer with 150 mM NaCl, (3) 10 mM HEPES with 10 mM NaCl, 20 μM $CaCl_2$ and 80 μM $MgCl_2$, and (4) 10 mM HEPES buffer with 150 mM NaCl, and 1 mM $CaCl_2$ (all chemicals were purchased through Sigma–Aldrich and used as received). The pH of all buffered solutions were adjusted with NaOH to a final pH of 7.4. All buffers where filtered through a 0.22 μm filter and stored at 4 °C.

2.2. Preparation of BSA solutions

BSA solutions contained 0.1 mg/mL of protein in the desired buffer. The BSA was prepared in one of four ways: (1) native BSA in which a 0.1 mg/mL BSA solution was prepared at 4 °C and stored at 4 °C overnight, (2) heat induced denatured BSA in which a 0.1 mg/mL BSA solution was prepared at 60 °C and stored in a 60 °C water bath overnight, (3) reduced BSA in which a 0.1 mg/mL BSA solution was prepared with 710 mM β-ME at 4 °C and stored at 4 °C overnight, and (4) reduced and denatured BSA in which a 0.1 mg/mL BSA solution was prepared with 710 mM β-ME at 60 °C and stored in a 60 °C water bath overnight. All samples were centrifuged prior to use at 15,570 × *g* for 25 min (Allegra 25R centrifuge) to remove any protein aggregates. All were used immediately after final preparation. The BSA stock solution was stored at 4 °C and used within a week. The concentration of the different BSA preparations was determined using a Bradford Assay (BioRad) and confirmed by SDS-PAGE. BSA-TMR solutions were prepared in an identical fashion as described above.

2.3. Liposome preparation

The procedure used to make small unilamellar vesicles (SUVs) via bath sonication was adapted from the recommended procedure described by Avant Polar Lipids (the lipid manufacturer). Lipid films were prepared by placing a chloroform solution of the desired mol/mol lipid ratio into a round bottom sample vial fitted with a Teflon top and the chloroform gently evaporated under a stream of dry nitrogen over 12 h. All samples contained 0.5 mol% Liss Rhod-PE. LMVs (large multilamellar vesicles) were prepared by hydrating the lipid films in the buffer of interest and gently swirling the solution at room temperature until the lipids were removed from the sides of the sample vial. The resulting opalescent solution had a final total lipid concentration of 4.5 mM. SUVs were formed by sonicating the solution for 30 min at 60 °C, which caused the solution to turn from opalescent to translucent. Samples containing POPC were stored at 4 °C and used within 3 days of preparation. Samples containing DMPC were use the same day they were prepared. All samples were centrifuged at 15,570 × *g* for 25 min immediately prior to use (Allegra 22R centrifuge). 'Single component' lipid samples contained 99.5% POPC or DMPC and 0.5% Liss Rhod-PE. 'Negatively charged' lipid mixtures contained 79.5% POPC, 20% Brain-PS, and 0.5% Liss Rhod-PE or 66.2% POPC, 33.3% POPG, and 0.5% Liss Rhod-PE. 'Cushioned' lipid samples contained 98.1% POPC, 1.4% PEG2000-PE,

and 0.5% Liss Rhod-PE. Liposomes made in the presence of β-ME were prepared by the same method as described above but with increasing concentrations of β-ME (0.1 mM, 10 mM, 140 mM, 710 mM).

2.4. Hydrophilic treatment of coverslips

Procedures used here are similar to those described previously (Davis et al., 2007; Poudel et al., 2011). Briefly, borosilicate coverslips (25 mm diameter for FRAP experiments or 12 mm diameter for AFM experiments; VWR) were first rinsed with nanopure water and hydrophilically treated by gentle agitation in a solution containing 20.0 mL of 5% NH_4OH and 20.0 mL of 4% H_2O_2 at 80–90 °C for 20 min. The solution was then decanted, and the coverslips were rinsed with copious amounts of water. The coverslips were then treated with gentle agitation in a solution containing 20.0 mL of 0.4 mM HCl and 20.0 mL of 4% H_2O_2 at 80–90 °C for 20 min. The solution was then decanted, and the coverslips were rinsed with water. The coverslips were then dried under a stream of dry nitrogen. Finally the coverslips were placed in a UV–ozone generator for 30 min prior to use.

2.5. Preparation of solid supported lipid bilayers for FRAP measurements

Supported lipid bilayers were formed through vesicle fusion as described earlier (Davis et al., 2007; Poudel et al., 2011). For this, a 50 μL aliquot of the SUVs was deposited onto the center of a mounted coverslip that was fitted with a parafilm® gasket containing a 10 mm diameter hole cut into its center and incubated for 30 min at 37 °C. The sample was then rinsed 10 times with fresh buffer (50 μL per rinse) to remove any excess lipid and 50 μL of fresh buffer was placed on top of the lipid bilayer. For samples containing BSA, a 50 μL aliquot of the BSA solution was placed onto the center of a mounted coverslip (described above), followed by a 25 min incubation at 37 °C. The sample was then rinsed 5 times (50 μL aliquots) with fresh buffer. Next, a 50 μL aliquot of the SUVs was placed on top of the coverslip containing the BSA and allowed to incubate for 30 min at 37 °C. After the final incubation step, the sample was rinsed 10 times with fresh buffer (50 μL per rinse) to remove any excess liposomes and 50 μL of fresh buffer was places on top of the membrane. All optical experiments were performed immediately after sample preparation.

2.6. Preparation of samples for AFM measurements

A 50 μL aliquot of the BSA solution was placed onto the center of a mounted coverslip, followed by a 25 min incubation at 37 °C. The sample was then rinsed 5 times with fresh buffer (50 μL per rinse). Excess rinsing buffer was removed and samples were thoroughly dried using a rapid stream of nitrogen. AFM images of samples prepared in this way were uniform over the sample surface, showed no signs of surface tension damage, and no signs of residual surface moisture. All experiments were performed immediately after sample preparation.

3. Experimental

3.1. Fluorescence microscopy

All fluorescence measurements were made using an Olympus IX71 fluorescence microscope that utilized a Hg:Xe lamp that was first passed through a 555 nm bandpass filter (25 nm FWHM; Chroma Technologies; S555/25x), reflected through a microscope objective (Olympus Apo 100x 1.45 N/A) with a dichroic mirror (multi-wave length; Chroma Technologies; 86016bs), and focused onto the sample. The emitted light was collected by the objective, passed through the dichroic mirror, and then passed through a 605 nm bandpass filter (40 nm FWHM_Chroma Technologies; S605/40m) before being imaged onto a Hamamatsu ORCAII CCD camera. All data collection and analysis were achieved using the Advanced Metamorph software suite (Olympus, Inc.).

3.2. FRAP measurements

A two-photon FRAP apparatus was built based on the design of Kubitscheck et al. (Kubitscheck et al., 1996) and has been described earlier (Poudel et al., 2012). Briefly, an Olympus IX71 fluorescence microscope equipped with a 1.45 N/A apochromatic 100× microscope objective along with a Hg:Xe arc lamp was used to monitor the fluorescence recovery, and a Spectra-Physics Titanium: Sapphire laser tuned to 780 nm (Mia–Tia; 100 MHz repetition rate, 80 fs FWHM pulse widths) was used to bleach the sample. The laser was attenuated to 30 mW average power. The shutters were synchronized and data was collected using the Advanced Metamorph software suite (Olympus, Inc.). All experiments were performed at room temperature (measured to be 18 °C) and the sample temperature was monitored with a silicon temperature sensor (diode; DT-470-SD). Data analysis was performed using a combination of the Advanced Metamorph software suite (Olympus, Inc.), IGOR 6.0 pro, and MATLAB (Mathworks Inc.).

To calculate the lateral diffusion coefficients associated with the recovery of the labeled lipids the following equation was used:

$$D = \left(\frac{\omega^2}{4t_{1/2}}\right)\gamma_D$$

where ω is the FWHM of the Gaussian profile of the focused beam, $t_{1/2}$ is the time for the bleached spot to recover half of its final intensity, and γ_D is a correction factor that depends on the bleaching time and the geometry of the laser beam (Axelrod et al., 1976). The value of γ_D was 1 for our experiments.

3.3. AFM measurements

Samples were imaged in ambient air using a Digital Instruments Nanoscope IIa AFM with a silicon tip operating in intermittent contact mode. Images were leveled by zero-order "flatten" filtering followed by first-order plane subtraction and line streak removal.

3.4. Dynamic light scattering

Dynamic light scattering was used to determine the sizes of the SUVs (DynaPro Titan Dynamic Light Scattering; Wyatt Technology Corp.). In these experiments, liposomes were prepared as described above, then diluted by 5 or 10 fold, and placed in a 1.5 mm quartz cuvette. The laser power was adjusted to keep the intensity around 50,000 cps. Measurements consisted of 20 consecutive 5 s scans. Data were analyzed using the manufacturer-supplied software (Dynamics 6.7.3). The average radii and size distribution was calculated using the regulation algorithm provided.

4. Results

4.1. Size distribution of liposomes under varying sample conditions

Dynamic light scattering (DLS) was used to verify the formation of SUVs and measure their size distribution under different sample conditions. This was especially important for liposomes made in the presence of β-ME because there is little known about the effect of β-ME on liposome formation and stability. DLS was also used to

Table 1
Results from DSL experiments show that the average liposome sizes increase with β-ME concentration for all lipid combinations except POPC/Brain-PS. The liposomes were composed of POPC, POPC/Brain-PS, POPC/PEG2000-PE, and DMPC. Measurements were made in 10 mM HEPES at pH 7.4 and performed at room temperature. Values recorded with and without β-ME.

Lipid combination	[β-ME]/mM	Average radius/nm
POPC	0	33.3 ± 2.3
	0.1	33.4 ± 2.7
	10	39.5 ± 3.3
	140	38.3 ± 3.6
	710	65.0 ± 8.53
POPC/brain-PS	0	19.4 ± 1.1
	0.1	20.1 ± 1.9
	10	20.8 ± 1.6
	140	23.1 ± 0.7
	710	22.8 ± 2.2
POPC/PEG2000-PE	0	60.2 ± 5.5
	0.1	62.0 ± 5.5
	10	75.5 ± 7.7
	140	79.5 ± 2.8
	710	81.8 ± 8.2
DMPC	0	17.1 ± 0.9
	0.1	19.9 ± 1.8
	10	19.9 ± 1.7
	140	22.3 ± 2.6
	710	56.5 ± 4.1

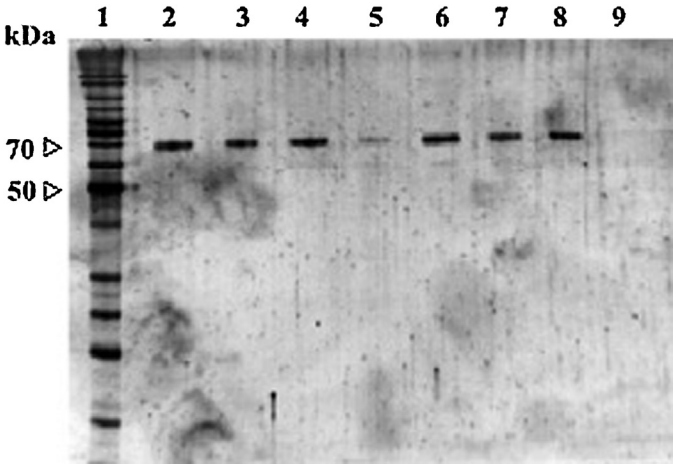

Fig. 1. SDS-PAGE Analysis of BSA under different denaturing conditions and ionic strengths shows no fragmentation but decreased concentration in reduced-denatured samples. The figure above is a 12% acrylamide SDS-PAGE of BSA samples prepared in 10 mM HEPES pH 7.4 (lanes 2–5) and 10 mM PBS 150 mM NaCl (lanes 6–9). Lanes 2 and 6 corresponds to native BSA, lanes 3 and 7 corresponds to heat denatured BSA, lanes 4 and 8 corresponds to reduced BSA and lanes 5 and 9 corresponds to reduced-denatured BSA. The BSA samples were compared against a protein ladder (lane 1).

measure SUV size distribution at elevated temperatures. Table 1 contains a summary of the results from this study. All lipid mixtures used in this study formed SUVs when sonicated in the different buffers listed above. Also, all lipid mixtures formed SUVs in the presence of β-ME (up to 710 mM). In general, SUVs containing DMPC formed the smallest liposomes followed closely by SUVs containing Brain-PS, then POPC liposomes. The largest were liposomes that contained 1.4 mol% PEG-2000-PE.

For liposome preparations in 10 mM HEPES, the sizes were within the expected value ranges for SUVs prepared using sonication (Bunjes, 2005; Vojta et al., 2005), and the average radius of the liposomes containing 1.4% PEG2000-PE in POPC was in agreement with reported values using a freeze–thaw technique (Diaz et al., 2008). Samples were also made in the presence of β-ME and incubated for 1 h at 23 °C or for 2 h at 60 °C in order to determine if the SUVs could withstand high concentrations of β-ME and to test whether β-ME would act as a fusogenic agent. For liposomes composed of POPC and DMPC swelling was observed over the concentration range from 0.1 mM to 140 mM. At 710 mM β-ME, both POPC and DMPC liposomes showed a dramatic increase in average size growing to more than twice their original value. POPC/Brain-PS liposomes also displayed some minor swelling, but seemed to be largely resistant to any dramatic effects caused by the addition of β-ME even at high concentrations (710 mM β-ME). Liposomes composed of 1.4 mol% PEG2000-PE in POPC displayed minor swelling at 0.1 mM β-ME and substantial swelling in liposome size from 10 mM to 710 mM β-ME. Moreover, once formed no significant changes were observed in the size distribution after 24 h or after incubating the samples at 60 °C for 2 h for all samples.

4.2. Concentrations and stability of BSA solutions before and after each sample preparation

BSA can precipitate out of solution as it ages and when treated with β-ME at 60 °C. Because of this, Bradford assays were performed to quantify (or estimate) the concentration of BSA after each sample preparation and SDS-PAGE was performed to confirm that BSA did not fragment. Native, reduced (β-ME), and denatured (heat) BSA samples gave very little precipitate after centrifugation and the Bradford Assay confirmed that the BSA concentrations were close to 0.10 mg/mL (the starting concentration). For reduced-denatured BSA samples there was noticeable precipitate after centrifugation in low ionic strength buffers and significant precipitate formation with high ionic strength buffers. Moreover, Bradford assays revealed that the concentrations of reduced-denatured BSA samples were decreased by as much as 25% in low ionic strength buffers (i.e., 10 mM HEPES) and below 1.25 μg/mL (the detection limit of the micro assay) in high ionic strength buffers (i.e., 10 mM phosphate 150 mM NaCl).

SDS:PAGE analysis confirmed the results from the Bradford assay and shows that BSA does not fragmented during the course of chemical reduction and heat denaturation. The results are displayed in Fig. 1. Lanes 2, 3, 4, and 5 are native, heat denatured, reduced, and reduced-heat denatured BSA, respectively, in low ionic strength buffer. Lanes 6, 7, 8, and 9 are native, heat denatured, reduced, and reduced-heat denatured BSA, respectively, in high ionic strength buffer. The samples were prepared using a standard SDS:PAGE prep that included incubation with a Laemmli Sample Buffer (BioRad Inc.), 710 mM β-ME, and SDS at 100 °C for 10 min. It should be noted that the SDS prevents protein precipitation. All samples, except for the reduced and denatured BSA sample at high ionic strength, displayed a band at 66 kD indicating that no fragmentation occurred. The absence of a band in lane 9 is consistent with the observation that the BSA precipitates out of solution when it is reduced and denatured in a high ionic strength buffer. Also, the band in lane 5 has much lower intensity. This too is consistent with the result that reduced and denatured BSA in low ionic strength buffer also has a lower solubility than native, reduced, or heat denatured samples Fig. 1.

4.3. Bilayer formation depends on the state of BSA used to passivate the surface

Fluorescence microscopy and fluorescence recovery after photobleaching (FRAP) was used to determine whether liposomes would fuse and form lipid bilayers on BSA-passivated surfaces. Liposomes that attach to a surface without forming a continuous

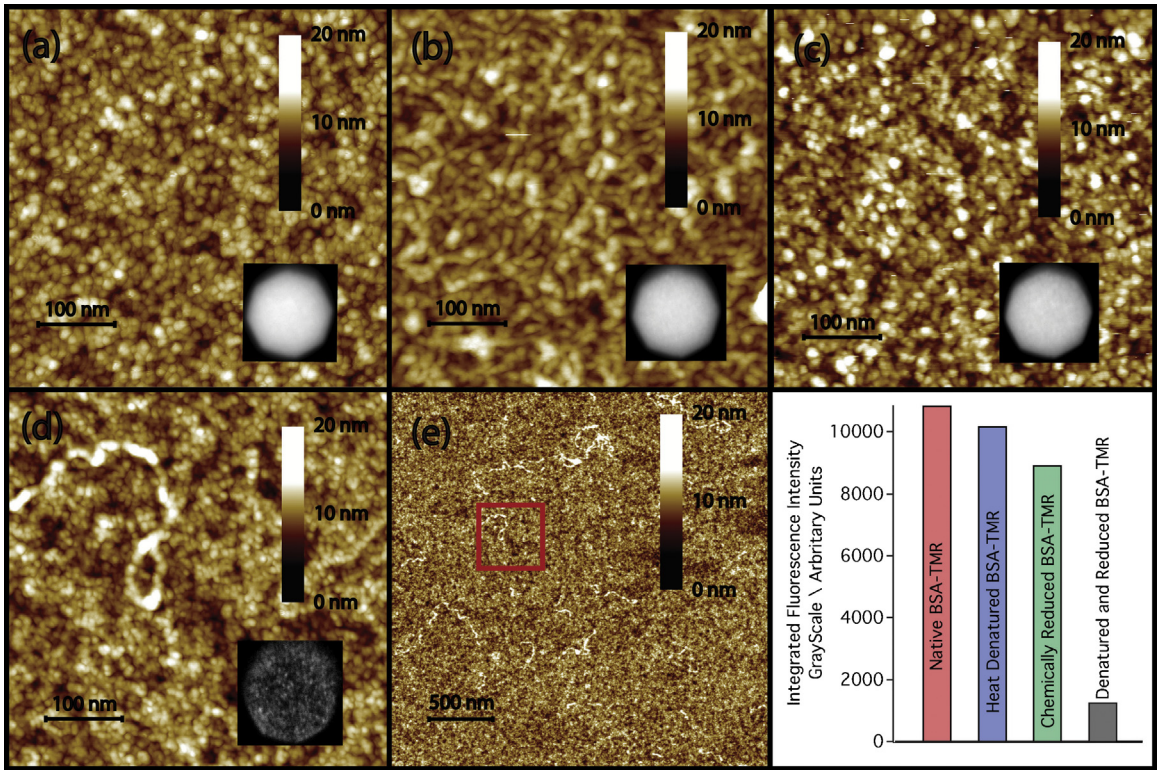

Fig. 2. AFM images show very little increase in surface roughness for BSA passivated samples. Incomplete surface coverage is observed for reduced-denatured samples. (a) A glass substrate that was passivated with native BSA prepared in 10 mM HEPES, (b) a glass substrate passivated with BSA prepared in 10 mM HEPES and reduced with 710 mM β-ME, (c) a glass substrate passivated with heat denatured BSA prepared in 10 mM HEPES, (d) a glass substrates that was passivated with BSA that was both reduced by 710 mM β-ME and heat denatured in 10 mM HEPES. The red box in (d) indicates the area in the magnified image depicted in (e). The insets are fluorescence micrographs of BSA-TMR passivated substrates prepared under identical conditions as the BSA samples. The contrast for each fluorescence image in a, b, and c were the same but the contrast in d was set 10× more sensitive. The bar graph shows the relative integrated intensities for each fluorescence micrograph. (For interpretation of the references to color in this figure legend, the reader is referred to the web version of this article.)

bilayer give rise to granulated fluorescence images and FRAP with little to no recovery (Fig. 3). Liposomes that form a continuous lipid bilayer give rise to fluorescence images devoid of granular structure and have high FRAP recoveries and relatively fast recovery times (Fig. 4). Moreover, it is known that negatively charged liposomes will only form bilayers in the presence of divalent cations (Ca^{2+}, Mg^{2+}, etc.).

In this study, it was observed that zwitterionic liposomes composed of DMPC, POPC, and POPC/PEG-PE all formed planar lipid bilayers on bare substrates, on substrates coated with native BSA, and on substrates treated with BSA that was both reduced and denatured (Fig. 4; Table 2). These same liposomes adsorbed to substrates coated with heat denatured or reduced BSA did not form bilayers but give rise to surfaces with tightly packed intact vesicles that give rise to granular fluorescence images and absolutely no FRAP recovery (Fig. 3). The choice of buffer did not affect whether a bilayer was formed but did have a small effects on the measured diffusion coefficient (see Table 2). In general, higher ionic strength buffers and BSA passivation resulted in slightly slower diffusion coefficients. The diffusion coefficients on bare hydrophyillically treated glass are all within the range of literature values (Albertorio et al., 2005; Castellana and Cremer, 2006; Diaz et al., 2008; Kapitza et al., 1984; Poudel et al., 2012; Wagner and Tamm, 2000). This is also true for negatively charged lipid bilayers (see below).

As expected, all negatively charged liposomes (POPC/Brain-PS and POPC/POPG) gave rise to granulated TIRFM images and near zero FRAP recoveries in the absence of a divalent cation indicating that liposomes adsorb to each substrate but fail to form lipid bilayers. In the presence of Ca^{2+}, the negatively charged liposomes follow the same trends as describe for the zwitterionic liposomes (above; table 2).

4.4. Surface roughness is largely unaffected by BSA passivation

Surface roughness and charge are critically important to bilayer formation. Surfaces passivated with reduced BSA and surfaces passivated with heat denatured BSA both promote vesicle adsorption but prevent the formation of a lipid bilayer. Therefore it was important to determine if increased surface roughness was present in the reduced BSA samples and in the heat denatured BSA samples. AFM studies were carried out in order to address this issue (Fig. 2). These experiments demonstrate that: (1) substrates treated with native BSA, reduced BSA, and heat denatured BSA thoroughly coated the glass substrate's surface (this was true for all buffer conditions), (2) the overall surface roughness was similar from sample to sample and was dominated by the underlying substrate, and (3) the reduced BSA and heat denatured BSA samples displayed aggregates that are a little larger and more heterogeneous than the native BSA samples (Fig. 2b and c), and (4) BSA that was heat denatured in addition to reduction with β-ME did not fully coat the glass substrate no matter the buffer and/or ionic strength. Instead, long strings and loop-like structures dotted the surface with large portions of the substrate not coated at all (Fig. 2d and e).

4.5. Incomplete surface coverage is observed for samples treated with reduced-denatured BSA

Fluorescence microscopy on hydrophilically treated glass substrates coated with BSA-TMR was used to confirm the surface

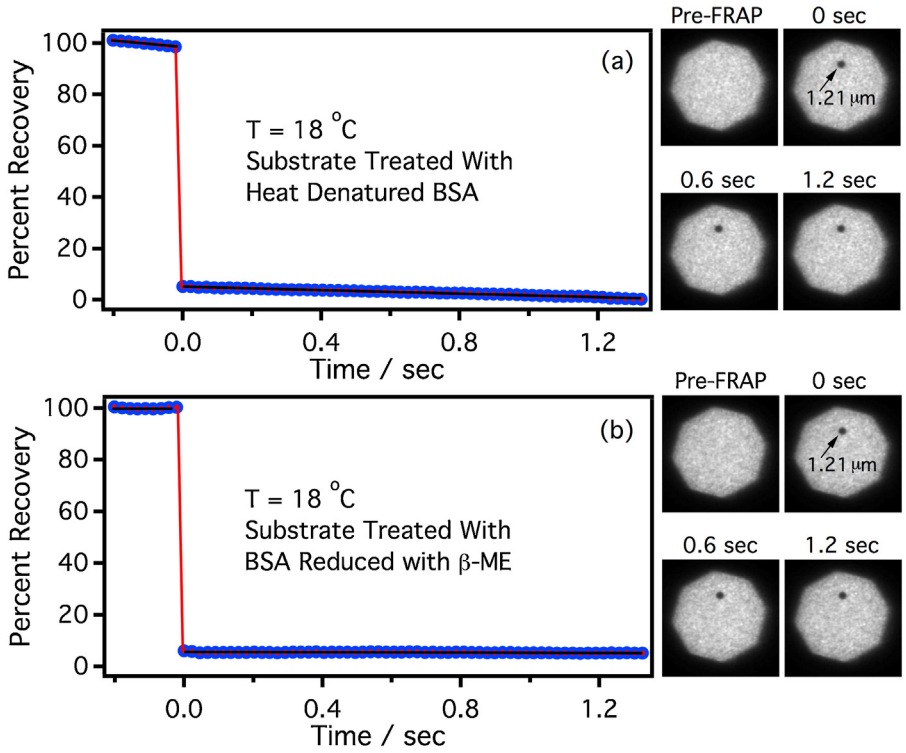

Fig. 3. FRAP recovery curves and fluorescence images demonstrate POPC vesicle adsorption on (a) a substrate treated with heat denatured BSA and (b) a substrates treated with BSA that was reduced with β-ME. All experiments were performed at 18 °C.

coverage of each BSA treated substrate at the microscale. The results appear as insets in fig. 2a, b, c, and d. The polygon shape of the fluorescence image is the result of a field stop inserted into the excitation arm of the fluorescence microscope to better visualize relative fluorescence intensity from the samples. The polygons were 15 microns by 15 microns. The contrast for fig. 2a, b, and c were the same but the contrast for fig. 2d had to be set 10× more sensitive in order to visualize the BSA-TMR adsorbed to the surface

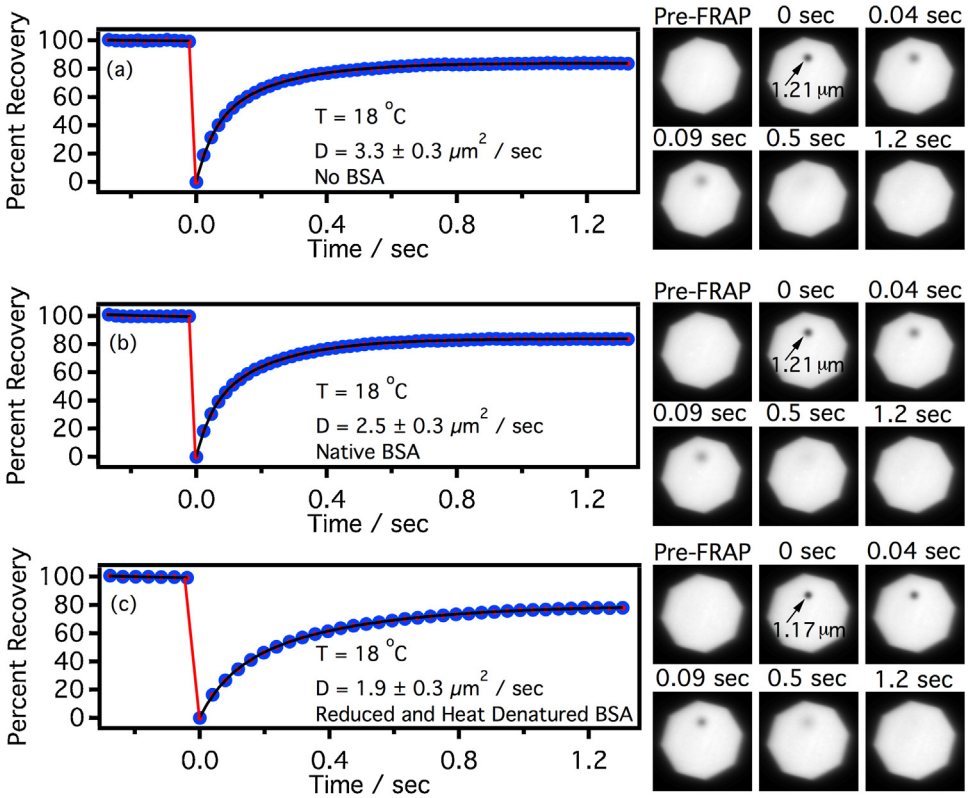

Fig. 4. FRAP recovery curves and fluorescence images demonstrate bilayer formation for POPC on (a) a hydrophilically treated glass substrate, (b) a substrate treated with native BSA, and (c) a substrate treated with BSA that was both heat denatured and reduced with β-ME. All experiments were performed at 18 °C.

Table 2
Diffusion coefficients and FRAP recoveries of supported lipid bilayers on a number of BSA passivated surfaces and in different buffers (all at pH 7.4). None = no BSA passivation, native = passivation with non-denatured BSA, RD = treated with BSA that has been both reduced with β-ME and heat denatured at 60 °C overnight. All data was collected at 18 °C. Note that at 18 °C DMPC is in its $P_{\beta'}$ phase, all other lipids are in their L_α phases.

Lipid combination	Buffer	Passivation	D (μm^2/sec)	Recovery (%)
POPC	10 mM HEPES	None	3.3 ± 0.3	84 ± 2
		Native	2.5 ± 0.3	82 ± 1
		RD	1.9 ± 0.2	79 ± 2
	10 mM HEPES/150 mM NaCl	None	3.0 ± 0.5	85 ± 2
		Native	2.5 ± 0.3	82 ± 2
		RD	1.4 ± 0.2	66 ± 3
	10 mM HEPES/150 mM NaCl/1 mM $CaCl_2$	None	2.8 ± 0.3	87 ± 2
		Native	2.1 ± 0.3	75 ± 1
		RD	1.7 ± 0.2	76 ± 3
	10 mM phosphate buffer/150 mM NaCl	None	2.8 ± 0.2	77 ± 1
		Native	2.1 ± 0.3	75 ± 1
		RD	1.1 ± 0.2	73 ± 4
POPC/Brain-PS	10 mM HEPES/150 mM NaCl/1 mM $CaCl_2$	None	1.9 ± 0.1	83 ± 2
		Native	1.7 ± 0.1	75 ± 4
		RD	1.4 ± 0.2	83 ± 3
	10 mM phosphate buffer/150 mM NaCl	None	1.5 ± 0.3	78 ± 5
		Native	1.2 ± 0.2	77 ± 2
		RD	1.1 ± 0.2	67 ± 3
POPC/PEG2000-PE	10 mM HEPES	None	1.4 ± 0.1	81 ± 2
		Native	1.1 ± 0.4	82 ± 2
		RD	0.55 ± 0.02	83 ± 2
	10 mM HEPES/150 mM NaCl	None	2.1 ± 0.2	75 ± 2
		Native	1.8 ± 0.2	75 ± 3
		RD	1.2 ± 0.2	73 ± 3
	10 mM phosphate buffer/150 mM NaCl	None	2.8 ± 0.4	78 ± 2
		Native	2.8 ± 0.3	80 ± 2
		RD	1.6 ± 0.2	69 ± 2
DMPC*	10 mM HEPES	None	0.10 ± 0.01	90 ± 3
		Native	0.10 ± 0.01	92 ± 2
		RD	0.10 ± 0.01	84 ± 4
	10 mM phosphate buffer/150 mM NaCl	None	0.21 ± 0.02	90 ± 4
		Native	0.10 ± 0.01	81 ± 5
		RD	0.05 ± 0.006	73 ± 3
POPC/POPG	10 mM HEPES/150 mM NaCl/1 mM $CaCl_2$	None	1.6 ± 0.3	85 ± 4
		Native	1.3 ± 0.2	82 ± 4
		RD	1.0 ± 0.1	73 ± 3
	10 mM phosphate buffer/150 mM NaCl	None	1.4 ± 0.1	82 ± 3
		Native	1.7 ± 0.1	76 ± 2
		RD	0.5 ± 0.1	69 ± 3

of the substrate. Fig. 2f is a bar graph showing the grayscale integrated intensities measure for each BSA-TMR-treated substrate. Images that display bright homogeneous intensities are indicative of thoroughly coated substrates while images that display dim heterogeneous intensities are indicative of low surface coverage. Each experiment was carried out as described in Section 3.1 with an integration time of 70 ms. These experiments are complimentary to the AFM experiments described above and confirm that 'native', chemically reduced, and heat denatured BSA-TMR thoroughly coat the surface while substrates treated with BSA-TMR that was both heat denatured and reduced only partially coats the surface.

5. Discussion

5.1. SUV formation in the presence of β-ME

In this study the disulfide bonds in BSA (there are 17) (Majorek et al., 2012) were reduced by the addition of β-ME and for this reason it was important to establish what effects β-ME could have on SUV and planar supported lipid bilayer formation. Apart from this immediate interest, β-ME is also used to decrease photochemical degradation in luminescence measurements (evident in FRAP studies) and as an oxygen scavenger in a wide range of other studies important to self-assembly, biomimetics, and soft materials research (Aitken et al., 2008; Hohng and Ha, 2004; Rasnik et al., 2006). The physical properties of β-ME are comparable to ethanol, which readily partitions into lipid bilayers, increases the area per lipid molecule, decreases the membrane thickness, decreases the overall surface tension in a lipid bilayer, and increases the interdigitation between adjacent lipid molecules (Ingolfsson and Andersen, 2011; Ly and Longo, 2004). These effects are known to increase the size of small unilamellar vesicles (SUVs), large unilamellar vesicles (LUVs), and giant unilamellar vesicles (GUVs) in the presence of ethanol (Komatsu et al., 1993; Ly and Longo, 2004; Zeng et al., 1993). One question addressed here is whether β-ME would have similar effects on SUVs and whether β-ME would prevent the formation of a lipid bilayer. Remarkably, SUVs and planar supported lipid bilayers will form in relatively high concentrations of β-ME. Moreover, FRAP recovery curves measured in the presence of β-ME gave identical results to samples free of β-ME. The only effect caused by the presence of β-ME seems to be on the size of the initially formed SUVs.

For systems composed of zwitterionic lipids, a considerable amount of swelling was observed with increasing concentration of β-ME (Table 1) similar to what is observed in the presence of

ethanol. It is reasonable to presume that the origin of this behavior is concomitant for the two molecules. But once the liposomes were formed, β-ME did not appear to cause smaller liposomes to fuse into larger ones, even when incubated for 24 h at room temperature or at elevated temperature (60 °C) for 2 h. Therefore we conclude that β-ME does not seem to be a fusogenic agent and liposomes can be stored in buffers containing β-ME for up to 24 h.

Another interesting result was that β-ME produced no observable effect on liposomes containing negatively charged lipids. These liposomes proved to be quite resistant to swelling with increasing concentrations of β-ME and displayed no increase in polydispersity over time and elevated temperature.

5.2. Passivation and bilayer formation

Native, reduced, and heat denatured BSA all coat the substrate equally well and the surface roughness was small and mainly dominated by the underlying substrate. While surfaces treated with reduced or heat denatured BSA resulted in structures that were a little larger and slightly more heterogeneous (on average) than native BSA, these topographical differences seem rather small. Yet, substrates treated with native BSA readily promote the formation of lipid bilayers through vesicle fusion and those treated with reduced or heat denatured BSA did not.

From literature accounts, the formation of lipid bilayers through vesicle fusion seems to be affected by at least two different factors associated with the solid support, surface roughness and net surface charge (Anderson et al., 2009; Castellana and Cremer, 2006; Cha et al., 2006; Cremer and Boxer, 1999). If charged liposomes are used, a third necessary condition is the presence of a divalent cation (Ca^{2+} and Mg^{2+} are most commonly used). It has been shown in previous studies that a low surface roughness is necessary for bilayer formation via vesicle fusion. Moreover, it has also been shown that BSA will spread evenly (and thinly) onto a glass substrate when the solution concentration is kept low (Sweryda-Krawiec et al., 2004) and it has been demonstrated that bilayers will not form on BSA passivated substrates if the concentration of the BSA is above 0.2 mM (presumably because of increased surface roughness) (Diaz et al., 2008). In the current study, the BSA concentration was kept low ($\leq$0.1 mM) and AFM measurements show that BSA was evenly spread across the surface and contributed little to the overall surface roughness.

In another study, it was demonstrated that surface charge (either positive or negative) was critically important for lipid bilayer formation from zwitterionic liposomes (Cha et al., 2006) and it is well known that divalent cations (such as Ca^{2+} or Mg^{2+}) closely associate with a hydrophilically treated substrates and are critically important for bilayer formation if negatively charged liposomes are used. BSA in its native state seems to be ideally suited to meet these two electrostatic conditions in that it has a somewhat high negative surface charge and it is known to chelate Ca^{2+} at three specific binding sites (Cha et al., 2006) and possibly more Ca^{2+} in a non-specific fashion (Peters, 1995). In fact, 45% of all Ca^{2+} in blood serum is bound to serum albumin (Ca^{2+} concentration in serum is ~2.4 mM and serum albumin is present in ~0.6 mM) (Peters, 1995).

Since only minor surface topography changes are observed upon reduction or heat denaturing of BSA, we conclude that the most probable causes for the loss of bilayer formation is that (1) surface charge drops below a critical surface charge density (Cha et al., 2006), and (2) the loss of the strong Ca^{2+} chelation sites prevents bilayer formation from negatively charged liposomes. This seems reasonable because upon denaturation, the Ca^{2+} binding sites would disappear from BSA with loss of its tertiary structure and the surface charge could easily be reduced if fewer polar or charged groups are in solvent exposed areas.

5.3. Bilayers on surfaces treated with reduced and denatured BSA

When BSA is both heat and chemically denatured, it tends to form large aggregates and falls out of solution. This effect is exaggerated in buffers with high ionic strength. Because the solubility is so low, the BSA never fully coats the surface. Instead, long strings and loops of BSA dispersed about the solid support are observed in AFM experiments and small islands of BSA-TMR are observed in fluorescence imaging experiments. Because the surface is mostly bare, liposomes will still fuse to the solid support and form bilayers in a normal fashion. The only effect observed on the lipid bilayers is that the measured diffusion coefficients are always lower when reduced-denatured BSA dots the surface. We presume this is because the islands of denatured BSA block the lipids and thus recovery must occur by diffusion around the small, nanometer sized, obstructions.

6. Conclusions

Understanding the necessary conditions for bilayer formation was the motivation behind this study. The passivation of a glass or silica substrate with BSA is straightforward, but the self-assembly of a lipid bilayer on top of a BSA passivated surface can be quite finicky. We found that only freshly prepared BSA stored at 4 °C for less than a week would reliably facilitate the formation of lipid bilayers from SUVs. Moreover, denaturing BSA by either heat or β-ME will prevent the formation of a lipid bilayer but still sequester liposomes. AFM studies demonstrated that BSA passiviation did not cause a significant increase in surface roughness regardless of whether the BSA was native, reduced, or heat denatured. Therefore the loss of BSA's ability to facilitate bilayer formation must be caused by chemical and/or structural changes to BSA itself. With loss of ternary structure the strong Ca^{2+} binding sites are presumably lost and it seems quite likely that the surface charge density is reduced. The reduction of surface charge will affect whether a zwitterionic liposome will rupture and form a lipid bilayer and loss of Ca^{2+} binding sites will affect whether a negatively charged liposome will rupture to form a bilayer.

Conflict of interest

The authors declare that there are no conflicts of interest.

Transparency document

The Transparency document associated with this article can be found in the online version.

Acknowledgments

Support was provided by the Department of Energy Office of Basic Energy Science. Many thanks to Dr. K.W. Hipps for use of the Scanning Probe Microscopy center at WSU and to Dr. C. Kang for use of his DSL equipment and expertise. Washington State University is also acknowledged for its support.

References

Aitken, C.E., Marshall, R.A., Puglisi, J.D., 2008. An oxygen scavenging system for improvement of dye stability in single-molecule fluorescence experiments. Biophys. J. 94, 1826–1835.

Albertorio, F., Diaz, A.J., Yang, T., Chapa, V.A., Kataoka, S., Castellana, E.T., Cremer, P.S., 2005. Fluid and air-stable lipopolymer membranes for biosensor applications. Langmuir 21, 7476–7482.

Anderson, T.H., Min, Y., Weirich, K.L., Zeng, H., Fygenson, D., Israelachvili, J.N., 2009. Formation of supported bilayers on silica substrates. Langmuir 25, 6997–7005.

Axelrod, D., Koppel, D.E., Schlessinger, J., Elson, E., Webb, W.W., 1976. Mobility measurement by analysis of fluorescence photobleaching recovery kinetics. Biophys. J. 16, 1055–1069.

Bunjes, H., 2005. Characterization of solid lipid nano and microparticles. In: Nastruzzi, C. (Ed.), Lipospheres in Drug Targets and Delivery: Approaches, Methods, and Applications. CRC Press.

Castellana, E.T., Cremer, P.S., 2006. Solid supported lipid bilayers: From biophysical studies to sensor design. Surf. Sci. Rep. 61, 429–444.

Cha, T., Guo, A., Zhu, X.Y., 2006. Formation of supported phospholipid bilayers on molecular surfaces: role of surface charge density and electrostatic interaction. Biophys. J. 90, 1270–1274.

Chan, Y.H., Boxer, S.G., 2007. Model membrane systems and their applications. Curr. Opin. Chem. Biol. 11, 581–587.

Chung, M., Lowe, R.D., Chan, Y.H.M., Ganesan, P.V., Boxer, S.G., 2009. DNA-tethered membranes formed by giant vesicle rupture. J. Struct. Biol. 168, 190–199.

Cornell, B.A., Braach-Maksvytis, V.L., King, L.G., Osman, P.D., Raguse, B., Wieczorek, L., Pace, R.J., 1997. A biosensor that uses ion-channel switches. Nature 387, 580–583.

Cremer, P.S., Boxer, S.G., 1999. Formation and spreading of lipid bilayers on planar glass supports. J. Phys. Chem. B 103, 2554–2559.

Davis, R.W., Flores, A., Barrick, T.A., Cox, J.M., Brozik, S.M., Lopez, G.P., Brozik, J.A., 2007. Nanoporous microbead supported bilayers: stability, physical characterization, and incorporation of functional transmembrane proteins. Langmuir 23, 3864–3872.

Diaz, A.J., Albertorio, F., Daniel, S., Cremer, P.S., 2008. Double cushions preserve transmembrane protein mobility in supported bilayer systems. Langmuir 24, 6820–6826.

Elender, G., Kuhner, M., Sackmann, E., 1996. Functionalisation of Si/SiO_2 and glass surfaces with ultrathin dextran films and deposition of lipid bilayers. Biosens. Bioelectron. 11, 565–577.

Fruh, V., AP, I.J., Siegal, G., 2011. How to catch a membrane protein in action: a review of functional membrane protein immobilization strategies and their applications. Chem. Rev. 111, 640–656.

Goennenwein, S., Tanaka, M., Hu, B., Moroder, L., Sackmann, E., 2003. Functional incorporation of integrins into solid supported membranes on ultrathin films of cellulose: impact on adhesion. Biophys. J. 85, 646–655.

Han, X., Achalkumar, A.S., Bushby, R.J., Evans, S.D., 2009. A cholesterol-based tether for creating photopatterned lipid membrane arrays on both a silica and gold surface. Chemistry 15, 6363–6370.

Hartshorn, C.M., Jewett, C.M., Brozik, J.A., 2010. Molecular effects of a nanocrystalline quartz support upon planar lipid bilayers. Langmuir 26, 2609–2617.

Hohng, S., Ha, T., 2004. Near-complete suppression of quantum dot blinking in ambient conditions. J. Am. Chem. Soc. 126, 1324–1325.

Ingolfsson, H.I., Andersen, O.S., 2011. Alcohol's effects on lipid bilayer properties. Biophys. J. 101, 847–855.

Jelinek, R., Silbert, L., 2009. Biomimetic approaches for studying membrane processes. Mol. Biosyst. 5, 811–818.

Johnson, J.M., Ha, T., Chu, S., Boxer, S.G., 2002. Early steps of supported bilayer formation probed by single vesicle fluorescence assays. Biophys. J. 83, 3371–3379.

Johnson, S.J., Bayerl, T.M., Mcdermott, D.C., Adam, G.W., Rennie, A.R., Thomas, R.K., Sackmann, E., 1991. Structure of an adsorbed dimyristoylphosphatidylcholine bilayer measured with specular reflection of neutrons. Biophys. J. 59, 289–294.

Kapitza, H.G., Ruppel, D.A., Galla, H.J., Sackmann, E., 1984. Lateral diffusion of lipids and glycophorin in solid phosphatidylcholine bilayers. The role of structural defects. Biophys. J. 45, 577–587.

Kaufmann, S., Papastavrou, G., Kumar, K., Textor, M., Reimhult, E., 2009. A detailed investigation of the formation kinetics and layer structure of poly(ethylene glycol) tether supported lipid bilayers. Soft Matter 5, 2804–2814.

Keller, C.A., Glasmastar, K., Zhdanov, V.P., Kasemo, B., 2000. Formation of supported membranes from vesicles. Phys. Rev. Lett. 84, 5443–5446.

Kendall, J.K., Johnson, B.R., Symonds, P.H., Imperato, G., Bushby, R.J., Gwyer, J.D., van Berkel, C., Evans, S.D., Jeuken, L.J., 2010. Effect of the structure of cholesterol-based tethered bilayer lipid membranes on ionophore activity. Chemphyschem 11, 2191–2198.

Kim, J., Kim, G., Cremer, P.S., 2001. Investigations of water structure at the solid/liquid interface in the presence of supported lipid bilayers by vibrational sum frequency spectroscopy. Langmuir 17, 7255–7260.

Komatsu, H., Guy, P.T., Rowe, E.S., 1993. Effect of unilamellar vesicle size on ethanol-induced interdigitation in dipalmitoylphosphatidylcholine. Chem. Phys. lipid. 65, 11–21.

Kubitscheck, U., TschodrichRotter, M., Wedekind, P., Peters, R., 1996. Two-photon scanning microphotolysis for three-dimensional data storage and biological transport measurements. J. Microsc.-Oxford 182, 225–233.

Kuhner, M., Sackmann, E., 1996. Ultrathin hydrated dextran films grafted on glass: preparation and characterization of structural, viscous, and elastic properties by quantitative microinterferometry. Langmuir 12, 4866–4876.

Kunding, A., Stamou, D., 2006. Subnanometer actuation of a tethered lipid bilayer monitored with fluorescence resonance energy transfer. J. Am. Chem. Soc. 128, 11328–11329.

Lipowsky, R., Seifert, U., 1991a. Adhesion of membranes – a theoretical perspective. Langmuir 7, 1867–1873.

Lipowsky, R., Seifert, U., 1991b. Adhesion of vesicles and membranes. Mol. Cryst. Liquid Cryst. 202, 17–25.

Ly, H.V., Longo, M.L., 2004. The influence of short-chain alcohols on interfacial tension, mechanical properties, area/molecule, and permeability of fluid lipid bilayers. Biophys. J. 87, 1013–1033.

Majewski, J., Wong, J.Y., Park, C.K., Seitz, M., Israelachvili, J.N., Smith, G.S., 1998. Structural studies of polymer-cushioned lipid bilayers. Biophys. J. 75, 2363–2367.

Majorek, K.A., Porebski, P.J., Dayal, A., Zimmerman, M.D., Jablonska, K., Stewart, A.J., Chruszcz, M., Minor, W., 2012. Structural and immunologic characterization of bovine, horse, and rabbit serum albumins. Mol. Immunol. 52, 174–182.

Merzlyakov, M., Li, E., Gitsov, I., Hristova, K., 2006. Surface-supported bilayers with transmembrane proteins: role of the polymer cushion revisited. Langmuir 22, 10145–10151.

Munro, J.C., Frank, C.W., 2004. In situ formation and characterization of poly (ethylene glycol)-supported lipid bilayers on gold surfaces. Langmuir 20, 10567–10575.

Murray, D.H., Tamm, L.K., Kiessling, V., 2009. Supported double membranes. J. Struct. Biol. 168, 183–189.

Peters, T., 1995. All About Albumin: Biochemistry, Genetics, and Medical Applications, first ed. Academic Press.

Poudel, K.R., Keller, D.J., Brozik, J.A., 2011. Single particle tracking reveals corralling of a transmembrane protein in a double-cushioned lipid bilayer assembly. Langmuir 27, 320–327.

Poudel, K.R., Keller, D.J., Brozik, J.A., 2012. The effect of a phase transition on single molecule tracks of Annexin V in cushioned DMPC assemblies. Soft Matter 8, 11285–11293.

Rabe, M., Verdes, D., Seeger, S., 2011. Understanding protein adsorption phenomena at solid surfaces. Adv. Colloid. Interface Sci. 162, 87–106.

Rasnik, I., McKinney, S.A., Ha, T., 2006. Nonblinking and long-lasting single-molecule fluorescence imaging. Nat. Meth. 3, 891–893.

Reimhult, E., Hook, F., Kasemo, B., 2002. Temperature dependence of formation of a supported phospholipid bilayer from vesicles on SiO_2. Phys. Rev. E 66, .

Reimhult, E., Hook, F., Kasemo, B., 2003. Intact vesicle adsorption and supported biomembrane formation from vesicles in solution: Influence of surface chemistry, vesicle size, temperature, and osmotic pressure. Langmuir 19, 1681–1691.

Reviakine, I., Brisson, A., 2000. Formation of supported phospholipid bilayers from unilamellar vesicles investigated by atomic force microscopy. Langmuir 16, 1806–1815.

Richter, R.P., Berat, R., Brisson, A.R., 2006. Formation of solid-supported lipid bilayers: an integrated view. Langmuir 22, 3497–3505.

Richter, R.P., Him, J.L.K., Brisson, A., 2003. Supported lipid membranes. Mater. Today 6, 32–37.

Rigaud, J.L., Levy, D., 2003. Reconstitution of membrane proteins into liposomes. Meth. Enzymol. 372, 65–86.

Sackmann, E., 1996. Supported membranes: scientific and practical applications. Science 271, 43–48.

Sackmann, E., Tanaka, M., 2000. Supported membranes on soft polymer cushions: fabrication, characterization and applications. Trend. Biotechnol. 18, 58–64.

Sumino, A., Dewa, T., Takeuchi, T., Sugiura, R., Sasaki, N., Misawa, N., Tero, R., Urisu, T., Gardiner, A.T., Cogdell, R.J., Hashimoto, H., Nango, M., 2011. Construction and structural analysis of tethered lipid bilayer containing photosynthetic antenna proteins for functional analysis. Biomacromolecules 12, 2850–2858.

Sweryda-Krawiec, B., Devaraj, H., Jacob, G., Hickman, J.J., 2004. A new interpretation of serum albumin surface passivation. Langmuir 20, 2054–2056.

Tanaka, M., Sackmann, E., 2005. Polymer-supported membranes as models of the cell surface. Nature 437, 656–663.

Tresset, G., 2009. The multiple faces of self-assembled lipidic systems. PMC Biophys. 2, 3.

Tribet, C., Vial, F., 2008. Flexible macromolecules attached to lipid bilayers: impact on fluidity, curvature, permeability and stability of the membranes. Soft Matter 4, 68–81.

Vojta, A., Scheuring, J., Neumaier, N., Mirus, O., Weinkauf, S., Schleiff, E., 2005. Determination of liposome size: a tool for protein reconstitution. Anal. Biochem. 347, 24–33.

Wagner, M.L., Tamm, L.K., 2000. Tethered polymer-supported planar lipid bilayers for reconstitution of integral membrane proteins: silane-polyethyleneglycol-lipid as a cushion and covalent linker. Biophys. J. 79, 1400–1414.

Wong, J.Y., Majewski, J., Seitz, M., Park, C.K., Israelachvili, J.N., Smith, G.S., 1999a. Polymer-cushioned bilayers. I. A structural study of various preparation methods using neutron reflectometry. Biophys. J. 77, 1445–1457.

Wong, J.Y., Park, C.K., Seitz, M., Israelachvili, J., 1999b. Polymer-cushioned bilayers. II. An investigation of interaction forces and fusion using the surface forces apparatus. Biophys. J. 77, 1458–1468.

Zeng, J., Smith, K.E., Chong, P.L., 1993. Effects of alcohol-induced lipid interdigitation on proton permeability in L-alpha-dipalmitoylphosphatidylcholine vesicles. Biophys. J. 65, 1404–1414.

Zhdanov, V.P., Kasemo, B., 2001. Comments on rupture of absorbed vesicles. Langmuir 17, 3518–3521.